Nitrogen Reduction by the Fe Sites of Synthetic [Mo3S4Fe] Cubes

Yasuhiro Ohki (ohki@scl.kyoto-u.ac.jp)
Kyoto University https://orcid.org/0000-0001-5573-2821
Kenichiro Munakata
Nagoya University
Ryota Hara
Nagoya University
Mami Kachi
Nagoya University
Keisuke Uchida
Nagoya University
Mizuki Tada
Nagoya University
Roger Cramer
University of Hawaii
Wmc Sameera
Hokkaido University
Tsutomu Takayama
Daido University
Yoichi Sakai
Daido University
Shogo Kuriyama
University of Tokyo
Yoshiaki Nishibayashi
University of Tokyo https://orcid.org/0000-0001-9739-9588
Kazuki Tanifuji
Kyoto University

Physical Sciences - Article

Keywords: nitrogen, fe sites, N2 reduction

Posted Date: May 13th, 2021

DOI: https://doi.org/10.21203/rs.3.rs-477541/v1

Version of Record: A version of this preprint was published at Nature on July 6th, 2022. See the published version at https://doi.org/10.1038/s41586-022-04848-1.

Title: Nitrogen Reduction by the Fe Sites of Synthetic [Mo_3S_4Fe] Cubes

Authors: Yasuhiro Ohki[1,*], Kenichiro Munakata[2], Ryota Hara[2], Mami Kachi[2], Keisuke Uchida[2], Mizuki Tada[2], Roger E. Cramer[3], W. M. C. Sameera[4], Tsutomu Takayama[5], Yoichi Sakai[5], Shogo Kuriyama[6], Yoshiaki Nishibayashi[6], and Kazuki Tanifuji[1]

Affiliations: [1] Institute for Chemical Research, Kyoto University, Gokasho, Uji 611-0011, Japan

[2] Department of Chemistry, Graduate School of Science, and Research Center for Materials Science, Nagoya University, Furo-cho, Chikusa-ku, Nagoya 464-8602, Japan

[3] Department of Chemistry, University of Hawaii, Honolulu, HI 96822-2275, United States

[4] Instituted of Low Temperature Science, Hokkaido University, Sapporo 060-0819, Japan

[5] Department of Chemistry, Daido University, Takiharu-cho, Minami-ku, Nagoya 457-8530, Japan

[6] Department of Applied Chemistry, School of Engineering, The University of Tokyo, Hongo 7-3-1, Bunkyo-ku, Tokyo 113-8656, Japan

Corresponding author: Email: ohki@scl.kyoto-u.ac.jp

Summary paragraph: N_2 fixation by Nature, which is a crucial process to supply bio-available forms of nitrogen, is performed by nitrogenase. This enzyme employs a unique transition metal-sulfur-carbon cluster as its active-site cofactor ([(*R*-homocitrate)$MoFe_7S_9C$], FeMoco),[1,2] and the sulfur-surrounded Fe atoms have been postulated to capture and reduce N_2.[3-6] Whereas synthetic counterparts of FeMoco, metal-sulfur clusters, have displayed binding of N_2 in a few examples,[7,8] the reduction of N_2 by any synthetic metal-sulfur clusters or even by the extracted form of FeMoco[9] have remained elusive despite a near-50-year history of research. Here we show that the Fe atoms in our synthetic [Mo_3S_4Fe] cubes[10,11] capture an N_2 molecule and catalyze N_2 silylation to form $N(SiMe_3)_3$ under treatment with excess Na and Me_3SiCl. These results exemplify the first catalytic N_2 reduction by a synthetic metal-sulfur cluster with an Fe center supported only by S ligands. This work demonstrates the N_2-reducing capability of Fe atoms in a S-rich environment, which Nature has selected to accomplish a similar purpose. This work also suggests some critical features for successful N_2 reduction by metal-sulfur compounds, which serve as clues to understand the origin of N_2 fixation on Earth.

Main Text

Nitrogen is an essential element to maintain every known form of life on Earth. Whereas the element is affluent in the atmosphere as N_2, only diazotrophs can fix this stable molecule into bio-available forms (*e.g.* NH_3). Other organisms consequently rely on products of the fixation process and limited pre-existing sources to afford necessary nitrogen. In this sense, N_2 fixation is one of the most crucial biocapacity bottlenecks on Earth. Key players of N_2 fixation are nitrogenase enzymes that reduce N_2 into NH_3. The most studied one of these, Mo-nitrogenase, employs a unique metal-sulfur-carbon cofactor described as [(*R*-homocitrate)$MoFe_7S_9C$] (FeMoco, Fig. 1)[1,2] and performs the catalytic reduction at ambient temperature and pressure. Since FeMoco is found only in nitrogenase, its chemical and physical properties have attracted significant interest concerning the desirable N_2-reducing activity. How FeMoco reduces N_2 has long been studied by biochemical analyses of the enzyme[3,12] and by structural and functional modeling of FeMoco with small-molecule complexes [13,14] and metal-sulfur clusters[15,16].

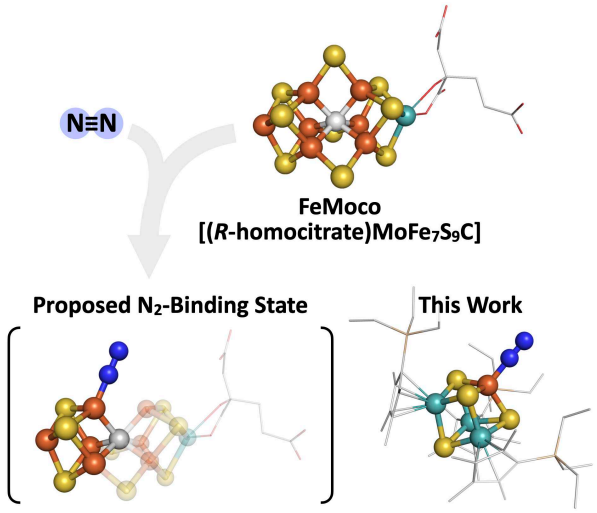

Fig. 1. One of the proposed N_2-binding states of FeMoco and an N_2-bound Mo-Fe-S cluster in this work.

While the structure of FeMoco has been identified clearly (Fig. 1), the detailed N_2-reducing mechanism remains elusive. A growing number of results suggest that FeMoco eliminates one of the μ_2-bridging S atoms and captures substrates at the produced vacant coordination sites on Fe atoms[4-6]. Analogously, a common approach to generate small-molecule N_2 complexes has been removal of a metal-bound ligand under reducing conditions. However, applying this method to available synthetic counterparts of the FeMoco, namely, metal-sulfur (M-S) clusters, has been challenging. As these clusters contain coordinative S atoms in their inorganic cores, a vacant metal site often attracts core S atoms of

different M-S clusters rather than N_2, which leads to aggregation[16]. Besides, the vacant site of a controlled N_2-reducing system must be selected from various and multiple metal atoms in these clusters. M-S clusters capture N_2 on rare occasions in this context[7,8]; nevertheless, a catalytic reduction of N_2 by these clusters remains unknown despite its relevance to the natural system. Our approach to overcome these hurdles implements a triangular $[Mo_3S_4]$ fragment bearing robust Mo-Cp^R bonds (Cp^R = C_5Me_5 (Cp*), $C_5Me_4SiMe_3$ (Cp^L) and $C_5Me_4SiEt_3$ (Cp^{XL}))[10,11] as a platform to structurally encumber and protect a fourth metal incorporated into the vertex (Fig. 1). This approach has allowed the observation of the capture and catalytic silylation of N_2 by the vertex Fe atoms of $[Mo_3S_4Fe]$ cubes. Results below demonstrate the first catalytic reduction of N_2 by M-S clusters with an Fe center supported only by S atoms.

In recent years, our laboratory reported the synthesis of various $[Mo_3S_4M]$ (M = transition metals) cubes derived from $[Mo_3S_4]$ platforms[10,11]. A Ti-derivative $[Cp^*_3Mo_3S_4Ti]$ captures and activates N_2 in the presence of KC_8, indicating that the $[Mo_3S_4Ti]$ cube is robust under reducing conditions and avoids undesirable aggregation[8]. Catalytic reduction of the bound N_2 was, however, not observed probably due to the strong Ti-N bond which inhibited product release. We then hypothesized that a softer Fe atom as found in the biological systems, instead of the harder Ti atom, may function more successfully to carry out N_2 reduction.

Treatment of our reported $[Mo_3S_4Fe]$ clusters, $[Cp^R_3Mo_3S_4FeCl]$ (Cp^R = Cp* (**1a**), Cp^L (**1b**), and Cp^{XL} (**1c**))[10,11] with strong reductants (KC_8 for **1a** and $Na(C_{10}H_8)$ for **1b** and **1c**) under N_2 in THF led to the formation of the corresponding N_2-clusters (Fig. 2a). The N_2 coordination mode varies depending on the bulkiness of the Cp^R ligands, so that a $[Mo_3S_4Fe]$ dimer bridged by N_2, $[\{Cp^*_3Mo_3S_4Fe\}_2(\mu\text{-}N_2)]^{2-}$ (**2a**), and monomers each bearing a terminal N_2 ligand, $[Cp^R_3Mo_3S_4Fe(N_2)]^-$ (Cp^R = Cp^L (**2b**), and Cp^{XL} (**2c**)), were obtained. The N_2 binding modes of **2a**-**c** were assigned primarily from the ^{15}N NMR spectra of $^{15}N_2$-labeled clusters. Cluster **2a** exhibited a single signal at δ –40.9 ppm as expected from the equivalent N atoms of the bridging $^{15}N_2$ (Supplementary Fig. 1). Conversely, **2b** and **2c** gave two signals at δ 22.0 and –5.3 ppm for **2b** and δ 22.6 and –5.7 ppm for **2c**, corresponding to the inequivalent *proximal* and *distal* N atoms in these molecules. Terminal N_2 binding in **2b** and **2c** was further confirmed by IR-active N–N stretches observed at 1896 and 1902 cm^{-1}, respectively, both of which exhibited a bathochromic shift upon $^{15}N_2$ labeling (Supplementary Figs. 7 and 8). Despite our efforts, no meaningful N–N stretch for **2a** was detectable via resonance-Raman or IR measurements, perhaps due to slightly broken symmetry of the N_2 binding mode. X-ray crystallographic analyses revealed the molecular structures of **2a** and **2c** (Figs. 2b and 2c). As mentioned, **2a** shows the conformation of a N_2-bridged $[Mo_3S_4Fe]$ dimer with an inversion center at the middle of the two N atoms, while **2c** is a monomeric cluster bearing a terminally bound N_2. The N–

N distances (1.151(4) Å for **2a** and 1.136(5) Å for **2c**) are in between those of *free* N_2 (1.098(1) Å) and N_2H_2 (1.252 Å), suggesting weakened N–N bond. Likewise, the N–N stretching frequencies of **2b** and **2c** are close to the lower end of those reported for N_2 complexes of Fe^{II} or Fe^{I},[17] and the activation levels are even comparable to an Fe^0-N_2 complex supported by S- and C-based ligands[18].

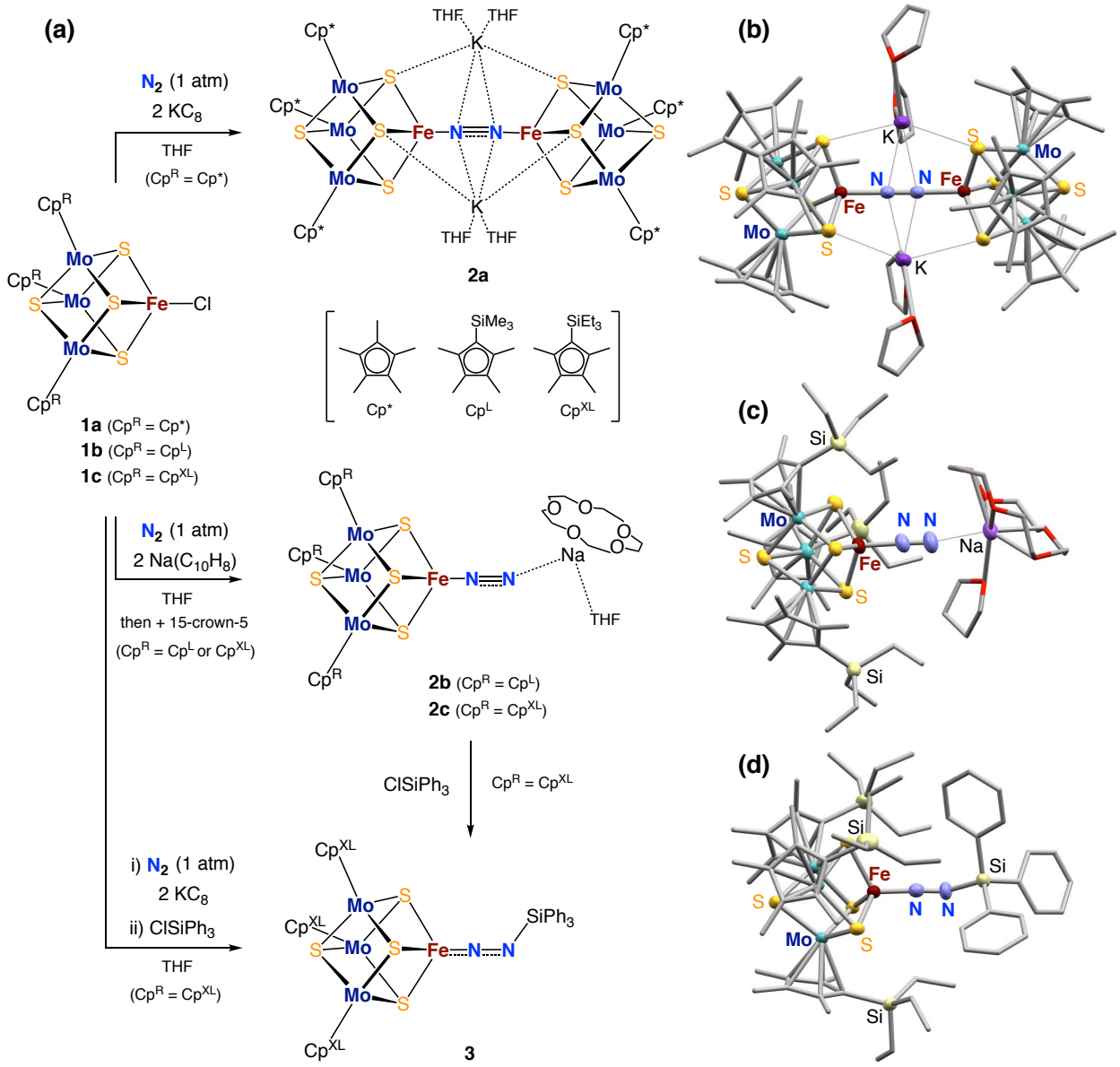

Fig. 2. (a) Synthetic schemes of N_2-bound [Mo_3S_4Fe] clusters **2a**-**2c**. Treatment of **1c** with KC_8 and $ClSiPh_3$ afforded **3**. (b-d) Structure of **2a**, **2c**, and **3**. For clarity, carbon and oxygen atoms are drawn as capped sticks.

Successful activation of N_2 at the Fe atoms of **2a**-**c** prompted us to pursue the catalytic reduction of N_2 using the [Mo_3S_4Fe] cubes. The clusters did not catalyze the conversion of N_2 into NH_3 giving at most

1.6 ± 0.1 equiv. NH_3 (per **2c**) under typical catalytic conditions[13,14,19]. Protonation of S atoms possibly occurs in this reaction and weakens Fe-S bonds to release a vertex Fe atom from $[Mo_3S_4Fe]$, in a relevant manner to degradation of the cubes under electrochemical oxidation[10,11]. Nonetheless, more importantly, we discovered that the Cl-clusters **1a**-**c** and N_2-clusters **2b** and **2c** all catalytically reduce N_2 to $N(SiMe_3)_3$ in the presence of excess Na and $ClSiMe_3$. A minimum of 122.9 ± 2.5 (per **1c**) and up to 248.0 ± 12.7 (per **1b**) equiv. of $N(SiMe_3)_3$ were generated after 100 hours under N_2 (1 atm) at room temperature (Table 1). While the cause of the differences in the activity of these complexes has not been conclusively identified at this point, we assume that the steric effects of the Cp^R ligands play a major role (*vide infra*) because the Cp^R substituents did not notably affect the redox behaviors of **1a**-**c** ($E_{1/2}$ ($[Mo_3S_4Fe]^{5+/4+}$) = –0.17 (**1a**), –0.19 (**1b**), and –0.24 (**1c**) V vs. Ag/Ag^+)[11].

Table 1. Catalytic reduction of N_2 into $N(SiMe_3)_3$ promoted by $[Mo_3S_4Fe]$ clusters.[a]

$$N_2\ (1\ atm) + 6\ Na + 6\ Me_3SiCl \xrightarrow[THF,\ r.t.\ 100\ h]{Catalyst} N(SiMe_3)_3$$

Entry	Catalyst	$N(SiMe_3)_3$ yield (equiv/catalyst)
1	**1a**	127.0 ± 28.3
2	**1b**	248.0 ± 12.7
3	**1c**	122.9 ± 2.5
4	**2b**	142.5 ± 13.1
5	**2c**	227.1 ± 33.3
6	**3**	258.3 ± 4.9
7	$Cp^*_3Mo_3S_4$	6.5 ± 1.2
8	$Cp^L_3Mo_3S_4$	9.6 ± 2.2
9	$Cp^{XL}_3Mo_3S_4$	12.9 ± 7.1

[a] 2000 equiv. each of Na and $ClSiMe_3$ were added to the catalyst in THF at room tempreture and stirred for 100 h under 1 atm N_2. Reactions by **2a** were not examined due to the low isolated yield and the lower performance of the Cp* (C_5Me_5) system. Yields represent the average of three runs.

The catalytic activities of **1b** and **2c** are higher than those of other Fe catalysts reported so far[20-22] and comparable to the most active Mo[23] and Co[24,25] catalysts for the homogeneous silylation of N_2. Similar to known systems, the catalytic reactions in THF concurrently formed $Me_3SiSiMe_3$, $Me_3SiOC_4H_9$, and $Me_3SiOC_4H_8SiMe_3$ as byproducts. These byproducts should originate from reactions of the trimethylsilyl

radical ·$SiMe_3$ with itself or THF solvent[25], as treatment of $ClSiMe_3$ with alkaline metals has been accepted to generate ·$SiMe_3$[23]. Although the THF solvent is much more abundant than the N_2 reactant, the selectivity for $N(SiMe_3)_3$ was high in the case of **1b** and reached 37.2% (entry 2). It is striking that neither the corresponding $[Mo_3S_4]$ platforms nor $FeCl_2$[20] provided $N(SiMe_3)_3$ at significant levels under the same conditions (entries 7-9). After a catalytic run using **1a**, a mass spectrum of the reaction mixture revealed $[Mo_3S_4Fe]$ cubes binding ring-opening products of THF (Supplementary Fig. 18), indicating sufficient stability of the cubic core during catalysis. These results suggest that the Fe center of each $[Mo_3S_4Fe]$ cube is the actual N_2-reducing site (Supplementary Scheme 1). More importantly, the observed catalysis displays the first example of N_2 reduction by Fe atoms in a S-rich environment, which was selected by Nature to achieve a similar aim.

Considering previous proposals for analogous reactions[23,25], we propose a mechanism for N_2-silylation by our $[Mo_3S_4Fe]$ cubes (Supplementary Scheme 1). In this pathway, we suppose that the Cl atom on Fe is removed by ·$SiMe_3$ to generate a vacant Fe site that binds N_2. In the resultant Fe-N_2 species, the more exposed *distal* N atom likely undergoes the first silylation to generate the Fe-$NNSiMe_3$ species. Further silylation and reduction would dissociate a hydrazido anion $[Me_3SiN–N(SiMe_3)_2]^–$, as theoretically proposed for Mo- and Co-catalyzed reactions[23,25]. Dissociation of the hydrazido anion can regenerate a vacant Fe site for the next catalytic cycle. Generation of the speculated Fe-$N(SiMe_3)$-$N(SiMe_3)_2$ species prior to dissociation of the hydrazido anion conforms to the proposed *alternating* mechanism in the N_2 reduction by nitrogenase[3].

The initial silylation of the N_2 ligand is arguably the most vital step in the N_2 reduction. To validate it, the *in situ* generated **2c** (from **1c** and 2.3 equiv. KC_8) was treated with 1.1 equiv. $ClSiPh_3$ to furnish a mono-silylated N_2 species ($[Cp^{XL}_3Mo_3S_4Fe(N_2SiPh_3)]$, **3**) in 20% yield (Figs. 2a and 2d). The same cluster **3** was alternatively generated from **2c** and $ClSiPh_3$ in C_6D_6 (Supplementary Fig. 5). The X-ray structure of **3** shows an elongated N-N distance (1.193(7) Å) from that found in the N_2-bound **2c** (1.136(5) Å), in accordance with a weakened N–N bond ($\nu_{N–N}$ = 1706 cm^{-1}). These values are close to previously reported Fe complexes bearing $[N_2SiR_3]$ ligands (Supplementary Table 5)[21,26,27]. While phenyl substituents on the Si atom of **3** differ from methyl groups employed in the catalytic process, the isolation of **3** supports the possible generation of an Fe-$NNSiMe_3$ analogue of **2c** in the catalytic cycle. This assumption was further reinforced by the successful catalytic N_2 silylation using **3** as the precursor, where 258.3 ± 4.9 equiv. of $N(SiMe_3)_3$ was formed (Table 1, entry 6).

Structural models of the N_2-bound clusters reveal that the Cp^R ligands surround the N_2 ligand and the $[Mo_3S_4Fe]$ cores (Fig. 3). The -$SiMe_3$ and -$SiEt_3$ groups of Cp^R ligands are forced into the space around

the Fe sites of [Mo_3S_4Fe] cubes (Fig. 3b and 3c) to minimize steric repulsion between the Cp^R ligands. Thus, the -SiR_3 groups efficiently offer steric protection of the [Fe-N_2] moiety and prevent dimerization of cubes through either an Fe-N_2-Fe bridge or an inter-cube Fe-S interaction. On the other hand, the less bulky Cp* ligands lead to a more exposed Fe site (Fig. 3a) and allow the approach of the Fe site of another [Mo_3S_4Fe] cube to give an Fe-N_2-Fe dimer. The bulkiness of Cp^R ligands should affect the catalytic activities as well, since we suggest that the first N-Si bond formation occurs at the *distal* N atom. In an Fe-N_2-Fe dimer, both N atoms are protected until one of the Fe-N interactions breaks to generate monomers. In the catalytic reactions using Fe-Cl cubes, chloride abstraction (initiation) is expected to be slower with the bulkier Cp^R ligands.

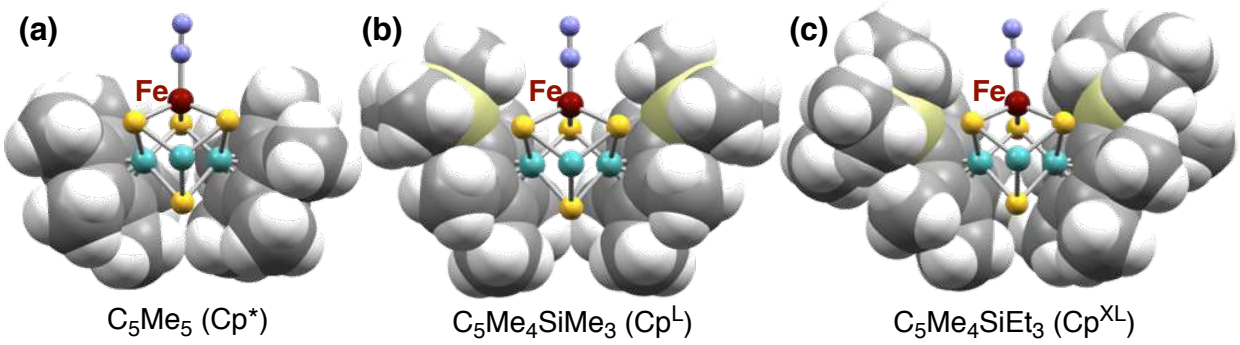

Fig. 3. Structural models of N_2-bound [Mo_3S_4Fe] clusters. Space-filling model is applied to two Cp^R ligands, while the other Cp^R is omitted to show the [Mo_3S_4Fe]-N_2 moiety. (a) and (c) were prepared from the crystal structures of **2a** and **2c**, while (b) was prepared via software using the Cl-bound cluster **1b**.

To better understand the properties of **2a**-**c** and **3**, Zero-field ^{57}Fe Mössbauer spectra were measured at 78 K using powdered crystals (Supplementary Fig. 10). The spectra were fitted as single quadrupole doublets with the following values of the isomer shift (δ) and the quadrupole splitting ($|\Delta E_Q|$): δ = 0.479(4) (**2a**), 0.410(2) (**2b**), 0.401(3) (**2c**), and 0.263(3) (**3**) mm/s; $|\Delta E_Q|$ = 1.258(8) (**2a**), 1.422(5) (**2b**), 1.466(5) (**2c**), and 0.906(5) (**3**) mm/s, respectively. The δ values of **2a**-**c** are lower than those of the precursors **1a**-**c** featuring Fe^{II} centers (δ = 0.555(2)–0.563(3) mm/s), even though **2a**-**c** are supposedly more reduced. A reduced Fe center typically displays a higher δ than an oxidized Fe in similar coordination environments, due to shielding of electrons in *s* orbitals by the increased 3*d* electron densities. This has also been verified for [Fe_4S_4] and [Fe_3S_4] clusters bearing thiolate ligands[28]. The observed opposite trend could be ascribed to the π back-donation from Fe to the N_2 ligand. As suggested from theoretical calculations, such increased covalency of the Fe-ligand bond leads to high electron density at the Fe nucleus and consequently, a low δ value[29]. Thus, while determination of the Fe oxidation state is not

straightforward, we tentatively assign the Fe centers in **2a**-**c** as close to Fe^{II} but only slightly reduced. Kohn-Sham frontier orbitals of optimized **2a** and **2c** reveal major contributions of Mo atoms in the occupied orbitals to store reducing equivalents (Supplementary Figs. 20-22). The DFT-calculated δ values of **2a**, **2c**, and **3** based on the crystal and optimized structures are qualitatively in agreement with the experimental data (Supplementary Table 9), supporting the utility of orbital analysis.

The covalent nature of Fe-N interaction can also rationalize the δ value of **3**. As illustrated by the N–N bond distance and N–N stretching frequency of the cluster, the silylation of the N_2 ligand has led to stronger back-donation from Fe and a shorter Fe–N distance (1.687(5) Å) than those of **2a** and **2c**. This is consistent with a highly covalent Fe–N interaction and does not contradict the decrease of the δ value in **3** compared to **2a**-**c**, implying a major contribution of a resonance structure of Fe=N=N–$SiPh_3$. A notably bent N–N–Si angle of **3** (133.4(5)˚), a linear Fe-N-N alignment (171.6(6) ˚), and computed Mayer bond orders (Fe–N, 1.49; N–N, 1.68) are in good agreement with a diazenido assignment. The effect of the Fe–N interaction on the δ variation of a series of clusters can be illustrated by a plot of their Fe–N bond distances versus δ values. The plot using data points of **2a**, **2c**, and **3** exhibits a pseudo-linear relationship as shown in Supplementary Fig. 19. Interestingly, similar relationships were also seen in $[(SiP^{i\text{-}Pr}_3)Fe(N_2)]^{0/-}$ and $[(SiP^{i\text{-}Pr}_3)Fe(N_2SiMe_3)]$ ($SiP^{i\text{-}Pr}_3$ = $Si(o\text{-}C_6H_4P^iPr_2)_3]^-$)[27], and $[LSnFe(N_2)]^{0/-}$ and $[LSnFe(N_2SiMe_3)]$ (L = $[N(o\text{-}(NCH_2P^iPr_2)(C_6H_4)_3]^{3-}$)[30], and regression lines from each series have nearly the same slope.

Overall, the above results represent the first catalytic N_2 reduction by a synthetic M-S cluster and suggest some critical features for successful N_2 reduction. Suppression of inter-molecular aggregation of M-S cores is crucial for a sufficiently long lifetime of N_2-bound species, while the enzyme buries the M-S core of FeMoco in a protein matrix to block such aggregation. Steric protection around the reaction site is important to enable the terminal binding of N_2, which facilitates the electrophilic attack at the *distal* N atom. Thus, appropriate choice of metal ligands is crucial, while the enzyme features an evolutionary developed protein backbone around FeMoco to achieve a similar purpose. Additional conditions for efficient catalysis are installation of a leaving group (Cl in this study and postulated μ_2-S in FeMoco) and robustness of the M-S cores under reducing conditions. While N_2 reduction to NH_3 or $N(SiMe_3)_3$ may have substantial mechanistic differences, our results confirm the novel N_2-reducing activity of Fe centers in S-rich environments, as is the case with FeMoco.

Data availability: X-ray data are available free of charge from the Cambridge Crystallographic Data Centre under reference numbers CCDC 2079174-2079176. All other experimental, spectroscopic, crystallographic, and computational data are included in the supplementary information.

Acknowledgements We thank T. Ohta (Sanyo-Onoda City Univ.) for attempted resonance-Raman measurements of **2a** and ^{15}N-labeled **2a**. We also acknowledge supercomputing resources at the Research Center for Computational Science at Okazaki and the Institute for Chemical Research at Kyoto University (Japan). This work was financially supported by Grant-in-Aids for Scientific Research (19H02733, 20K21207, 21H00021 for Y.O., 20H05671 and 20K21203 for Y. N., 20K15295 for S. K.) from the Japanese Ministry of Education, Culture, Sports, Science and Technology (MEXT), CREST grant (JPMJCR1541 for Y. N.) from JST, the Takeda Science Foundation, the Tatematsu Foundation, the Yazaki Memorial Foundation, and International Collaborative Research Program of ICR, Kyoto University.

Author contributions Y. O. designed the study. K. M., R. H., M. K. and K. U. conducted the experiments. M. T. participated in the discussion. Y. O. and K. T. interpreted the data. R. E. C. analyzed the single-crystal XRD data. W. M. C. S. collected and analyzed the computational data. T. T. and Y. S collected and analyzed the Mössbauer spectra. S. K. and Y. N. conducted experiments for ammonia synthesis. Y. O. and K. T. wrote the manuscript with input from all authors.

Competing interests: The authors declare no competing interests.

Additional information

Supplementary information is available for this paper

Correspondence and requests for materials should be addressed to Y.O.

References

1 Spatzal, T. et al. Evidence for interstitial carbon in nitrogenase FeMo cofactor. *Science* **334**, 940–940 (2011).

2 Lancaster, K. M. et al. X-ray emission spectroscopy evidences a central carbon in the nitrogenase iron-molybdenum cofactor. *Science* **334**, 974–977 (2011).

3 Seefeldt, L. C. et al. Reduction of substrates by nitrogenases. *Chem. Rev*. **120**, 5082–5106 (2020).

4 Spatzal, T., Perez, K. A., Einsle, O., Howard, J. B., Rees, D. C. Ligand binding to the FeMo-cofactor: Structures of CO-bound and reactivated nitrogenase. *Science* **345**, 1620–1623 (2014).

5 Sippel, D. et al. A bound reaction intermediate sheds light on the mechanism of nitrogenase. *Science* **359**, 1484–1489 (2018).

6 Kang, W., Lee, C. C., Jasniewski, A. J., Ribbe, M. W., Hu, Y. Structural evidence for a dynamic metallocofactor during N_2 reduction by Mo-nitrogenase. *Science* **368**, 1381–1385 (2020).

7 Mori, H., Seino, H., Hidai, M., Mizobe, Y. Isolation of a cubane-type metal sulfido cluster with a molecular nitrogen ligand. *Angew. Chem. Int. Ed*. **46**, 5431–5434 (2007).

8 Ohki, Y. et al. N_2 activation on a molybdenum–titanium–sulfur cluster. *Nat. Commun*. **9**, 3200 (2018).

9 Smith, B. E., Durrant, M. C., Fairhurst, S. A., Gormal, C. A., Grönberg, K. L. C., Henderson, R. A., Ibrahim, S. K., Le Gall, T., Pickett, C. J. Exploring the reactivity of the isolated iron-molybdenum cofactor of nitrogenase. *Coord. Chem. Rev.* **185-186**, 669-687 (1999).

10 Ohki, Y. et al. Cubane-type $[Mo_3S_4M]$ clusters with first-row groups 4–10 transition-metal halides supported by C_5Me_5 ligands on molybdenum. *Chem. Eur. J*. **24**, 17138–17147 (2018).

11 Ohki, Y. et al. Synthesis of $[Mo_3S_4]$ clusters from half-sandwich molybdenum(V) chlorides and their application as platforms for $[Mo_3S_4Fe]$ cubes. *Inorg. Chem*. **58**, 5230–5240 (2019).

12 Jasniewski, A. J., Lee, C. C., Ribbe, M. W., Hu, Y. Reactivity, mechanism, and assembly of the alternative nitrogenases. *Chem. Rev*. **120**, 5107–5157 (2020).

13 Chalkley, M. J., Drover, M. W., Peters, J. C. Catalytic N_2-to-NH_3 (or -N_2H_4) conversion by well-defined molecular coordination complexes. *Chem. Rev*. **120**, 5582–5636 (2020).

14 Tanabe, Y., Nishibayashi, Y. Comprehensive insights into synthetic nitrogen fixation assisted by molecular catalysts under ambient or mild con. *Chem. Soc. Rev*. (2021). doi:10.1039/d0cs01341b

15 Lee, S. C., Holm, R. H. The clusters of nitrogenase: synthetic methodology in the construction of weak-field clusters. *Chem. Rev*. **104**, 1135–1157 (2004).

16 Tanifuji, K., Ohki, Y. Metal-sulfur compounds in N_2 reduction and nitrogenase-related chemistry. *Chem. Rev*. **120**, 5194–5251 (2020).

17 Hazari, N. Homogeneous iron complexes for the conversion of dinitrogen into ammonia and hydrazine. *Chem. Soc. Rev.* **39**, 4044-4056 (2010).

18 Čorić, I., Mercado, B. Q., Bill, E., Vinyard, D. J., Holland, P. L. Binding of dinitrogen to an iron–sulfur–carbon site. *Nature* **526**, 96–99 (2015).

19 Anderson, J. S., Rittle, J., Peters, J. C. Catalytic conversion of nitrogen to ammonia by an iron model complex. *Nature* **501**, 84-87 (2013).

20 Yuki, M. et al. Iron-catalysed transformation of molecular dinitrogen into silylamine under ambient conditions. *Nat. Commun*. **3**, 1254 (2012).

21 Ung, G., Peters, J. C. Low-temperature N_2 binding to two-coordinate L_2Fe^0 enables reductive trapping of $L_2FeN_2^-$ and NH_3 generation. *Angew. Chem. Int. Ed*. **54**, 532–535 (2015).

22 Araake, R., Sakadani, K., Tada, M., Sakai, Y., Ohki, Y. $[Fe_4]$ and $[Fe_6]$ hydride clusters supported by phosphines: synthesis, characterization, and application in N_2 reduction. *J. Am. Chem. Soc*. **139**, 5596–5606 (2017).

23 Tanaka, H. et al. Molybdenum-catalyzed transformation of molecular dinitrogen into silylamine: Experimental and DFT study on the remarkable role of ferrocenyldiphosphine ligands. *J. Am. Chem. Soc.* **133**, 3498–3506 (2011).
24 Li, M., Gupta, S. K., Dechert, S., Demeshko, S., Meyer, F. Merging pincer motifs and potential metal-metal cooperativity in cobalt dinitrogen chemistry: efficient catalytic silylation of N_2 to $N(SiMe_3)_3$. *Angew. Chem. Int. Ed.* **60**, (2021). DOI: 10.1002/anie.202101387
25 Siedschlag, R. B. et al. Catalytic silylation of dinitrogen with a dicobalt complex. *J. Am. Chem. Soc*. **137**, 4638–4641 (2015).
26 Piascik, A. D. et al. Cationic silyldiazenido complexes of the Fe(diphosphine)$_2$(N_2) platform: structural and electronic models for an elusive first intermediate in N_2 fixation. *Chem. Commun.* **53**, 7657-7660 (2017).
27 Lee, Y., Mankad, N. P., Peters, J. C. Triggering N_2 uptake via redox-induced expulsion of coordinated NH_3 and N_2 silylation at trigonal bipyramidal iron. *Nat. Chem.* **2**, 558-565 (2010).
28 Rao, P. V., Holm, R. H. Synthetic analogues of the active sites of iron−sulfur proteins. *Chem. Rev*. **104**, 527–560 (2004).
29 Neese, F. Prediction and interpretation of the ^{57}Fe isomer shift in Mössbauer spectra by density functional theory. *Inorg. Chim. Acta* **337**, 181–192 (2002).
30 Dorantes, M. J., Moore, J. T., Bill, E., Mienert, B., Lu, C. C. Bimetallic iron-tin catalyst for N_2 to NH_3 and a silyldiazenido model intermediate. *Chem. Commun*. **56**, 11030–11033 (2020).

Figures

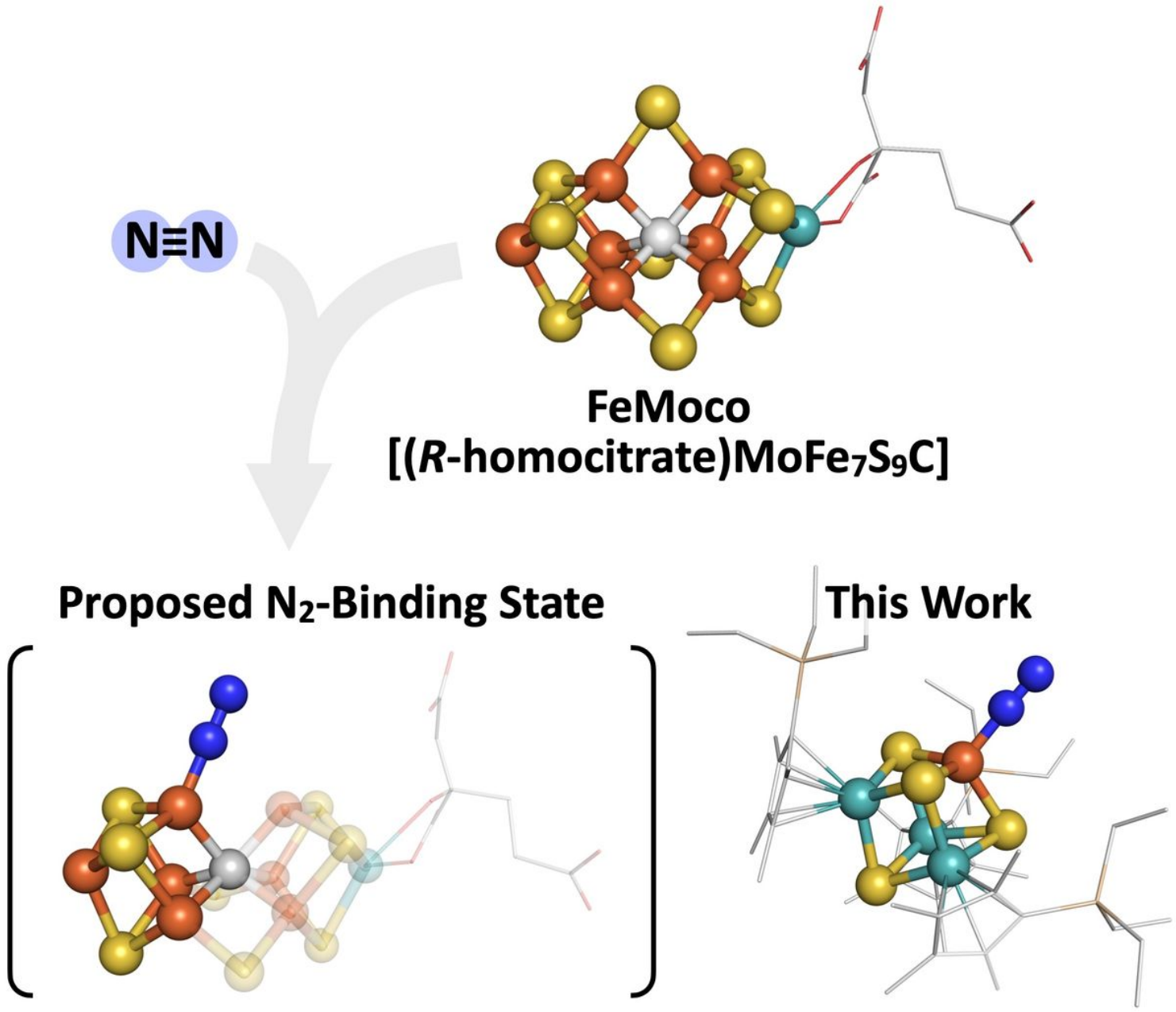

Figure 1

One of the proposed N2-binding states of FeMoco and an N2-bound Mo-Fe-S cluster in this work.

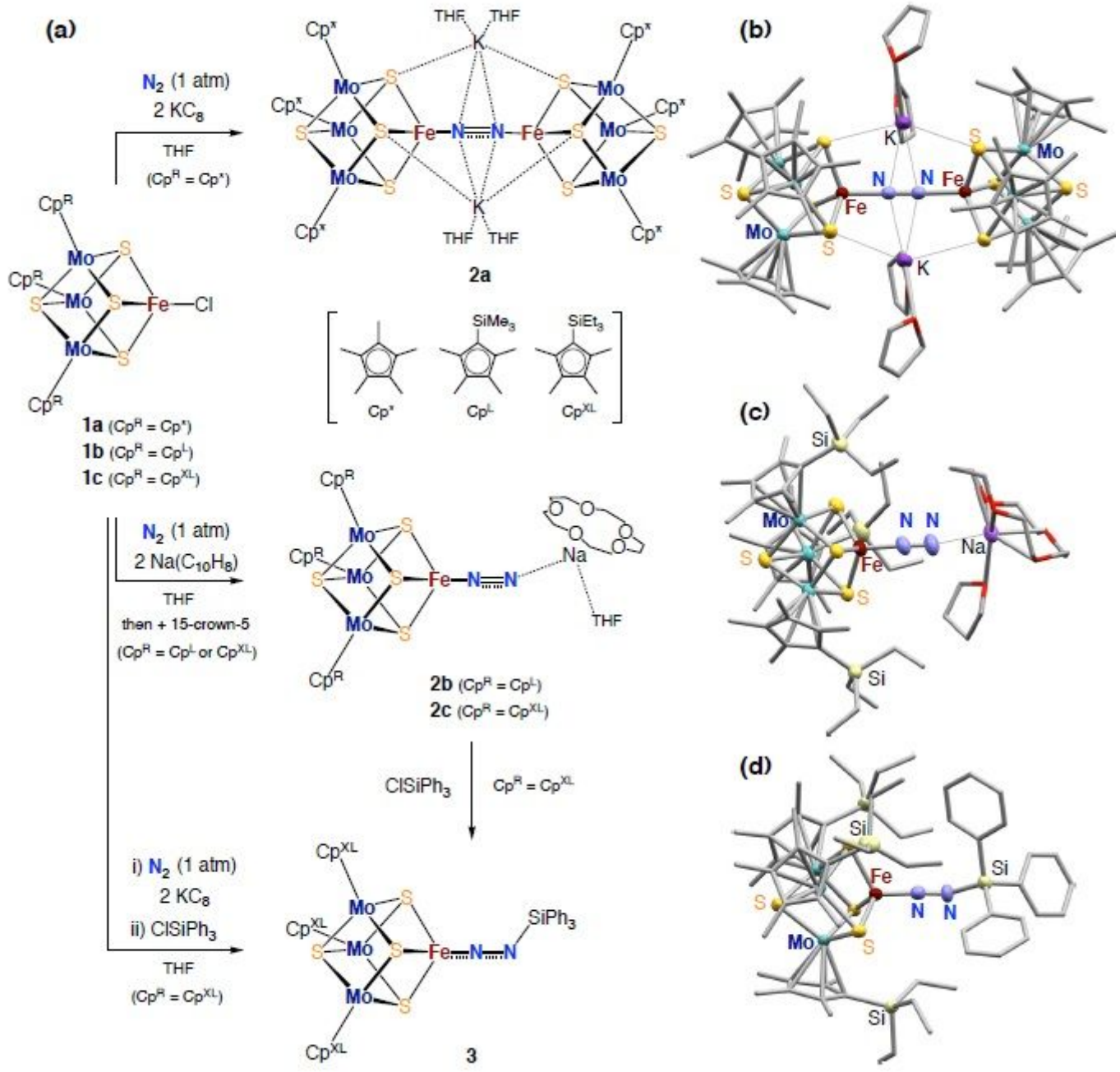

Figure 2

(a) Synthetic schemes of N2-bound [Mo3S4Fe] clusters 2a-2c. Treatment of 1c with KC8 and ClSiPh3 afforded 3. (b-d) Structure of 2a, 2c, and 3. For clarity, carbon and oxygen atoms are drawn as capped sticks.

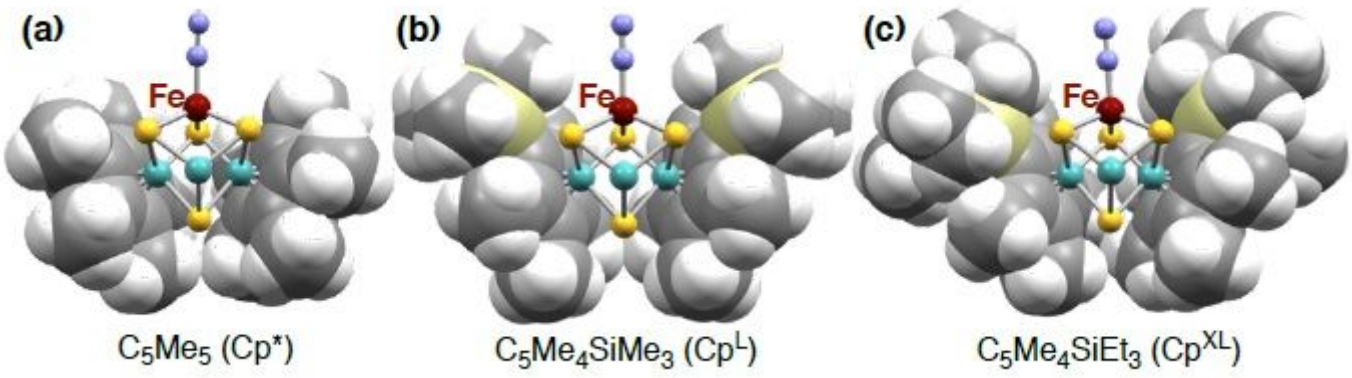

Figure 3

Structural models of N2-bound [Mo3S4Fe] clusters. Space-filling model is applied to two CpR ligands, while the other CpR is omitted to show the [Mo3S4Fe]-N2 moiety. (a) and (c) were prepared from the crystal structures of 2a and 2c, while (b) was prepared via software using the Cl-bound cluster 1b.

Supplementary Files

This is a list of supplementary files associated with this preprint. Click to download.

- Supprementaryinfo.pdf